Letters

Nose-to-Tail Modulation of Three-Phase 12*N* Switching-Cells Inverter for Zero Common Mode Voltage

Jiaxun Teng, *Student Member, IEEE*, Xiaofeng Sun, *Member, IEEE*, Zizhe Wang, Huanshuai Fu, Wei Zhao, Lei Qi, and Xin Li

***Abstract*—Aiming at a class of transformerless three-phase dc/ac inverters with *N* times of 12 switching-cells, this letter proposes a novel nose-to-tail modulation (NTM) method, which can realize zero common-mode voltage (CMV). The NTM algorithm places the driving pulses nose-to-tail of the six conversion units in the upper/lower arm, so as to realize the same number of units put into the upper and lower arms at any time. In addition, a dead-time compensation scheme achieving the elimination of narrow pulse CMV caused by dead time is also proposed for NTM. As a result, the zero CMV can be achieved. Although the proposed NTM slightly increases the modulation complexity, it is of great significance in CMV sensitive systems, such as grid-tied and motor drive systems. The effectiveness of the proposal is verified by experiments.**

***Index Terms*—Common mode voltage (CMV), nose-to-tail modulation (NTM), three-phase inverters.**

I. Introduction

THREE-PHASE dc/ac systems with 12*N* ($N = 1, 2, 3, \ldots$) switching cells have been widely used in practical projects, including three-phase parallel inverters (TPI) system shown in Fig. 1(a) [1], and modular multilevel converter (MMC)-based system shown in Fig. 1(b) [2]. One switching cell in TPI is a switch, and in MMC is a submodule (SM). Therefore, in line with the 12*N* switching cell in the TPI system means the inverters number is even, and in the MMC system means the number of SMs in one arm is even. The modulation technology of this class of topologies has always been a hot issue, and the basic modulation that is widely used includes sinusoidal pulse width modulation (SPWM), space vector pulse width modulation, and so on [3].

The transformerless design of the three dc/ac systems achieves the lightweight, but also brings series common-mode voltage (CMV) issues. In the motor drive system, the coupled current generated by CMV will harm the insulation layer of the motor, and the shaft current will accelerate the aging of bearing [4]. In the grid-tied system, the high-frequency leakage current caused by CMV will bring electromagnetic interference and affect the normal operation of other electric equipment [5]. Therefore, minimization CMV is great significance of dc/ac systems application. The definition of CMV can be obtained from the existing research [6] [7]

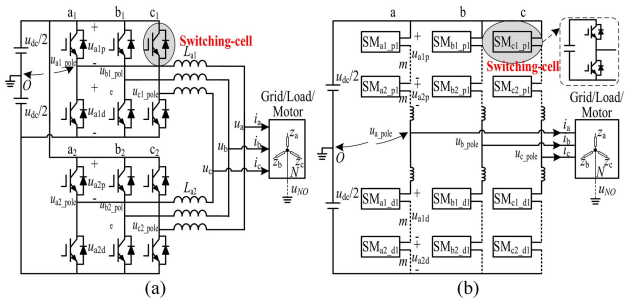

Fig. 1. Three-phase DC/AC systems with 12*N* switching cells. (a) TPI-based system. (b) MMC-based system.

$$\begin{cases} u_{\mathrm{CMV}} = u_{\mathrm{NO}} \\ \quad = \left(\begin{matrix} u_{\mathrm{a1\_pole}} + u_{\mathrm{b1\_pole}} + u_{\mathrm{c1\_pole}} \\ + u_{\mathrm{a2\_pole}} + u_{\mathrm{b2\_pole}} + u_{\mathrm{c2\_pole}} \end{matrix} \right) \Big/ 6 \text{ in TPI} \\ u_{\mathrm{CMV}} = u_{\mathrm{NO}} = (u_{\mathrm{a\_pole}} + u_{\mathrm{b\_pole}} + u_{\mathrm{c\_pole}})/3 \text{ in MMC} \end{cases} . \tag{1}$$

A five-level modulation strategy for dual-parallel inverters was proposed in [6], the additional vectors generated by which divided the original vector space into smaller regions, achieving the reducing of CMV. Du et al. [8] also discussed a CMV elimination method combining modulation algorithm and dual-segment three-phase motor design. Shen et al. [7] proposed a method to minimize the CMV of MMC grid-tied system based on the combination of a novel modulation method and feed-forward control, which can achieve the CMV reduction from 1/3 per unit to 1/6 m per unit, where 2 m is the number of MMC SMs in one arm. Edpuganti and Rathore [9] presented a synchronous optimal PWM technique of dual-MMC-based

Manuscript received 9 March 2023; revised 17 April 2023 and 15 May 2023; accepted 31 May 2023. Date of publication 7 June 2023; date of current version 22 September 2023. This work was supported in part by the Natural Science Foundation of Hebei Province under Grant E2021203162 and in part by the Key Research and Development Program of Hebei Province under Grant 19214405D. *(Corresponding authors: Wei Zhao; Xin Li.)*

The authors are with the Department of Electrical Engineering, Yanshan University, Qinhuangdao 066004, China (e-mail: tengjiaxun@qq.com; sxf@ysu.edu.cn; 1339099938@qq.com; q15710347220@163.com; zwysu@163.com; qil@ysu.edu.cn; yddylixin@ysu.edu.cn).

Color versions of one or more figures in this article are available at https://doi.org/10.1109/TPEL.2023.3282622.

Digital Object Identifier 10.1109/TPEL.2023.3282622

induction motor drives, which realized a good suppression effect on CMV.

This letter proposes a novel nose-to-tail modulation (NTM) method, which is a general CMV elimination modulation of a class of topologies, which are three-phase dc/ac topologies with $12N$ switching cells. NTM recombines and resorts the $12N$ units, and places the driving pulses nose-to-tail of the six switching cells in the upper/lower arm. Finally, the numbers of switch-ON/OFF cells of the upper and lower arms in the bridge converter are exactly the same at any time, thus realizing zero CMV of the system. The effect of dead time on NTM realization of zero CMV is also solved in this letter.

II. Principle of NTM

A. General Condition

For the two typical three-phase inverters shown in Fig. 1, to simplify the analysis process, it is assumed that the $N = 1$, that is, the number of inverters in Fig. 1(a) is 2, and the SMs in one arm of MMC in Fig. 1(b) is 2. Since each group of 12 switching cells can realize the zero CMV generated by this group, the elimination of CMV can be achieved in the same way in the system of $N \geq 2$. The pole voltages of both TPI and MMC can be obtained by Kirchhoff laws from Fig. 1

$$\begin{cases} u_{\mathrm{x1\_pole}} = (u_{\mathrm{x1d}} - u_{\mathrm{x1p}})/2 \\ u_{\mathrm{x2\_pole}} = (u_{\mathrm{x2d}} - u_{\mathrm{x2p}})/2 \end{cases} \text{in TPI} \\ u_{\mathrm{x\_pole}} = (u_{\mathrm{x1d}} - u_{\mathrm{x1p}})/2 + (u_{\mathrm{x2d}} - u_{\mathrm{x2p}})/2 \quad \text{in MMC} \tag{2}$$

where u_{x1p}, u_{x2p}, u_{x1d}, and u_{x2d} represent the voltage of upper and lower arms of phase-x (x stands for a, b or c), which is shown in Fig. 1(a) and (b). As can be seen from the (2), when N is 1 in both TPI and MMC, the pole voltage of MMC is equal to the sum of the pole voltages of the two inverters in TPI. The general expression of CMV in both TPI and MMC can be obtained from (1) and (2)

$$\begin{cases} u_{\mathrm{CMV}} = \\ \left[\begin{array}{l} (u_{\mathrm{a1d}} + u_{\mathrm{b1d}} + u_{\mathrm{c1d}} + u_{\mathrm{a2d}} + u_{\mathrm{b2d}} + u_{\mathrm{c2d}}) \\ -(u_{\mathrm{a1p}} + u_{\mathrm{b1p}} + u_{\mathrm{c1p}} + u_{\mathrm{a2p}} + u_{\mathrm{b2p}} + u_{\mathrm{c2p}}) \end{array} \right] \Big/ 12 \text{ in TPI} \\ u_{\mathrm{CMV}} = \\ \left[\begin{array}{l} (u_{\mathrm{a1d}} + u_{\mathrm{b1d}} + u_{\mathrm{c1d}} + u_{\mathrm{a2d}} + u_{\mathrm{b2d}} + u_{\mathrm{c2d}}) \\ -(u_{\mathrm{a1p}} + u_{\mathrm{b1p}} + u_{\mathrm{c1p}} + u_{\mathrm{a2p}} + u_{\mathrm{b2p}} + u_{\mathrm{c2p}}) \end{array} \right] \Big/ 6 \text{ in MMC} \end{cases} \tag{3}$$

From the (2), the CMV of TPI and MMC has a common feature, that is, both are defined as the difference of the sum of all lower arms voltage and the sum of all upper arms voltage. Therefore, the CMV of the system can be guaranteed to be zero by keeping the arms voltage difference to be zero.

Furthermore, the arms voltage corresponds exactly to the switch-ON/OFF signal, so the general condition of achieving zero CMV for both TPI and MMC at the modulation level is that the sums of switch-ON/OFF time of the upper and lower arms switching cells are same at any time, that is

$$u_{\mathrm{a1d}} + u_{\mathrm{a2d}} + u_{\mathrm{b1d}} + u_{\mathrm{b2d}} + u_{\mathrm{c1d}} + u_{\mathrm{c2d}} = u_{\mathrm{a1p}} + u_{\mathrm{a2p}} + u_{\mathrm{b1p}} + u_{\mathrm{b2p}} + u_{\mathrm{c1p}} + u_{\mathrm{c2p}}. \tag{4}$$

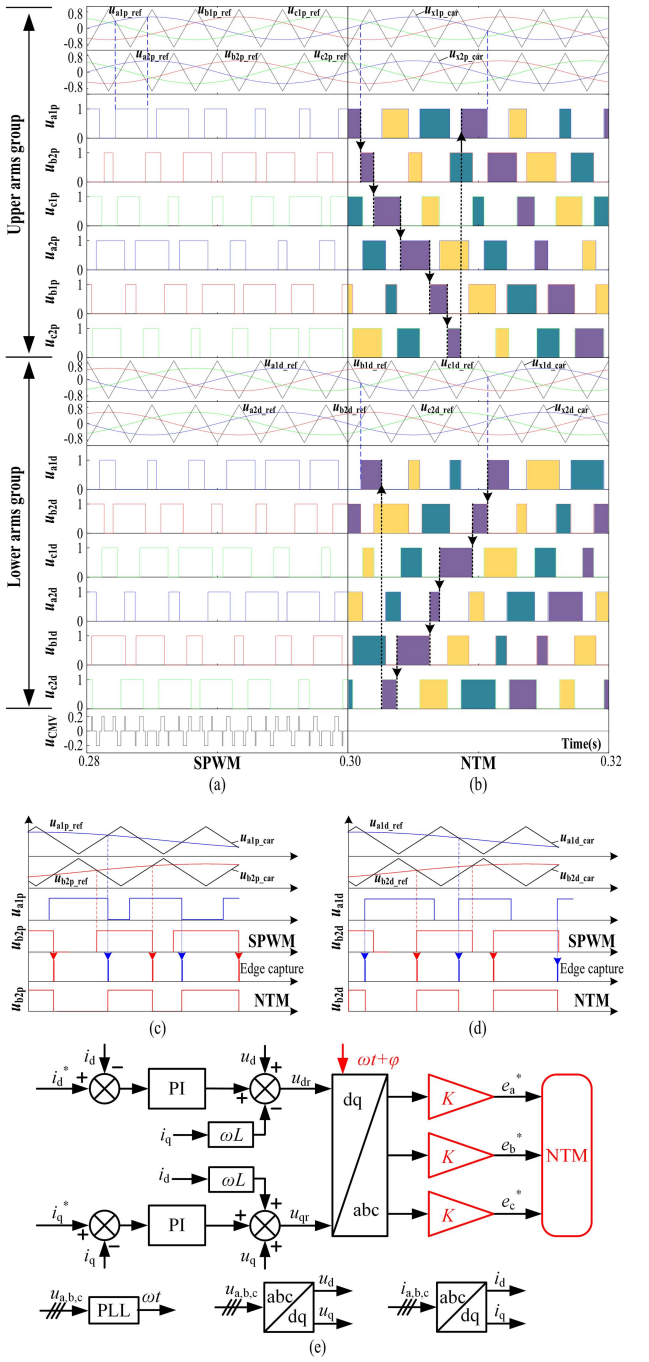

Fig. 2. Two modulation methods. (a) SPWM. (b) NTM. Pulse generation diagram of (c) upper arm and (d) lower arm of NTM. (e) Modified current loop control block with NTM.

B. NTM Implementation

The diagram of conventional SPWM is shown in Fig. 2(a), and due to the above general condition cannot be met, CMV will be generated to further harm the safe operation of the system in the application of TPI and MMC.

Based on the general condition of achieving zero CMV, this letter proposes an NTM method at the modulation level, as shown in Fig. 2(b). The switching cells are rearranged into upper and lower arms group. The new order is [u_{a1p}, u_{b2p}, u_{c1p}, u_{a2p},

u_{b1p}, u_{c2p}] in upper arms group and [$u_{a1d}, u_{b2d}, u_{c1d}, u_{a2d}, u_{b1d}$, u_{c2d}] in lower arms group. Within the arms group of TPI and MMC, the carrier phase differences between x1p and x2p, and x1d and x2d are 180°, which is exactly in line with the principle of carrier phase shift (CPS) modulation in MMC. On the basis, the carrier phase difference between x1p and x1d of the two arms groups is 180°. The detailed description of the switching logic is as follows.

The both two edges of switching signal of SPWM are determined by the carrier and modulating waveforms, and only one edge of switching signal of proposed NTM is determined by the carrier and modulating waveforms, and another edge is determined by the previous switching cell in the rearranged switching-cells groups, which are [u_{a1p}, u_{b2p}, u_{c1p}, u_{a2p}, u_{b1p}, u_{c2p}] in upper arms group and [u_{a1d}, u_{b2d}, u_{c1d}, u_{a2d}, u_{b1d}, u_{c2d}] in lower arms group.

For example, in the upper arms group, the switching signal of u_{b2p} takes the falling edge obtained by natural sampling of carrier and modulating waveforms as the switching-OFF signal, and the falling edge of the previous switching cell u_{a1p} as the switching-ON signal of u_{b2p}, as shown in the modulation diagram of upper arms group in Fig. 2(b) and (c), and the edges can be obtained by capture methods.

In the lower arms group, the switching signal of u_{b2d} takes the rising edge obtained by natural sampling as the switching-OFF signal, and the rising edge of the previous switching cell u_{a1d} as the switching-OFF signal of the latter switching cell u_{b2d}, as shown in the modulation diagram of lower arms group in Fig. 2(b) and (d).

Therefore, nose-to-tail switching signals are formed both in the upper and lower arms, so that the switching-ON/OFF cells of the upper and lower arms groups can be identical at any time, achieving zero CMV. Different from the natural sampling and regular sampling to obtain pulsewidth signals of traditional SPWM, in order to achieve zero CMV, the pulsewidth signals of the rearranged switching cells in the arms group are determined jointly by their own sampling and the previous switching cell. Therefore, the modulation principle of NTM encompasses changes in both phase shift φ and modulation ratio K. For instance, when considering grid-tied control of the current loop of an inverter, Fig. 2(e) illustrates a modified control loop with derived values for φ and K as analyzed below.

This letter analyzes the modulation principle of the proposed NTM by referring to the analysis process of the modulation principle of the traditional SPWM in [10]. Taking two adjacent switching cells a1p and b2p in upper arms group as an example, the modulation principle is shown in Fig. 3. Assuming that the initial phase of phase-a is 0, the modulation waves of phase-a and phase-b are

$$\begin{cases} u_{a1p\_ref} = m\cos(\omega t) \\ u_{b2p\_ref} = m\cos(\omega t - 2\pi/3) \end{cases} \tag{5}$$

where m is the modulation ration of SPWM. Since the frequency of carrier is much higher than the modulation wave, t_{a1_right} in Fig. 3 can be approximately half of t_{a1_SPWM}, that is, $t_{a1\_right} \approx t_{a1\_SPWM}/2$. Therefore, the switching-ON time of u_{b2p} with

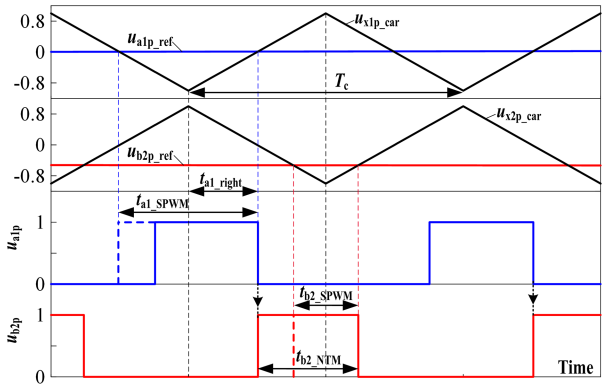

Fig. 3. Modulation principle of NTM.

NTM is

$$\begin{aligned} t_{b2p\_NTM} &= T_c/2 - t_{a1\_SPWM}/2 + t_{b2\_SPWM}/2 \\ &= T_c/2 - T_c\,(1/2 + u_{a1p\_ref}/2)/2 \\ &\quad + T_c\,(1/2 + u_{b2p\_ref}/2)/2 \\ &= T_c\left(1/2 + \sqrt{3}m\cos(\omega t - 2\pi/3 - \pi/6)\Big/4\right). \end{aligned} \tag{6}$$

The equivalent sinusoidal signal of switching cell b2p modulated by NTM can be further obtained, which of switching cells a1p and c1p can be obtained in the same way

$$\begin{cases} u_{a1p\_NTM} = \sqrt{3}m\cos(\omega t - \pi/6)/2 \\ u_{b2p\_NTM} = \sqrt{3}m\cos(\omega t - 2\pi/3 - \pi/6)/2 \\ u_{c1p\_NTM} = \sqrt{3}m\cos(\omega t + 2\pi/3 - \pi/6)/2 \end{cases}. \tag{7}$$

It can be seen from (7) that the modulation ration and phase of NTM are different from that of SPWM. The new modulation ratio is $K = 2/\sqrt{3}$ of original, and the phase lags $\varphi = \pi/6$, which are shown in Fig. 2(e).

C. Dead-Time Influence

The NTM proposed in this letter realizes zero CMV theoretically. However, as with other conventional modulation methods, narrow pulse CMV will still be formed due to the existence of dead time. Since the current will not mutate during switching-ON/OFF of the tube, the voltage at both ends of the switching tube is not synchronized with the gate signal, but is determined both by the current polarity and gate signal. Therefore, the dead time will cause a negative effect to the realization of zero CMV by NTM.

Fig. 4 shows the modulation principle of phase-a1 output voltage and gate signal at different current polarities. When the current polarity is positive, the level reversal of the output voltage is synchronized with the gate signal of the upper arm switching cell a1p, as shown in Fig. 4(a). When the current is negative, the output voltage synchronizes with the switching cell a1d of lower arm.

In the proposed NTM method, the gate signal of the upper and lower arms is connected nose-to-tail in accordance with [a1, b2,

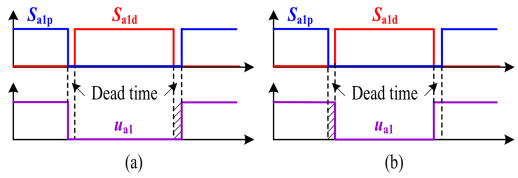

Fig. 4. Output voltage and gate signal of phase-a1 when the current polarity is (a) positive and (b) negative.

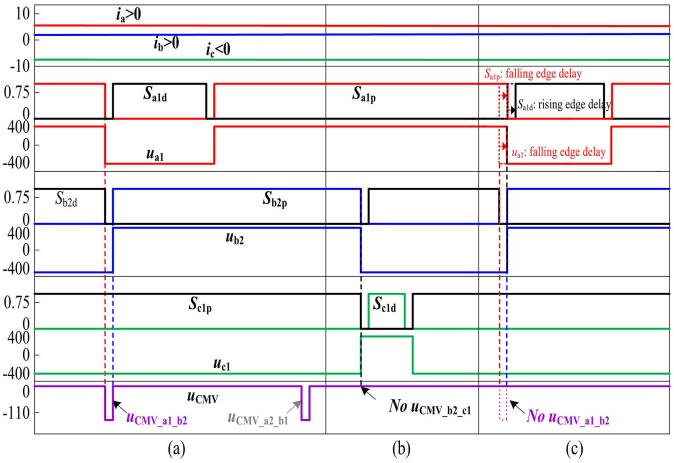

Fig. 5. Relationship between narrow pulse CMV and dead band when the output currents of two arms driven nose-to-tail are in (a) same direction [$i_{a1} > 0$, $i_{b2} > 0$] and (b) opposite direction [$i_{b2} > 0$, $i_{c1} < 0$]. (c) Dead-time compensation strategy of eliminating the narrow pulse CMV.

c1, a2, b1, c2]. It is possible to generate a narrow pulse CMV in the dead band of the two adjacent sets of gate signal connections, which is also related to the polarity of the currents. Taking the arms group [a1, b2, c1] and the currents polarity [$i_{a1} > 0$, $i_{b2} > 0$, $i_{c1} < 0$] as an example, the relationship between narrow pulse CMV and dead time and current polarity is discussed, as shown in Fig. 5. As shown in Fig. 5(a), when the output current polarity of two adjacent groups of arms is the same, that is, $i_{a1} > 0$ and $i_{b2} > 0$, the output voltage of phase-a1 and phase-b2 overlaps in the dead band, resulting in narrow pulse CMV. As shown in Fig. 5(b), when the output current polarity of two adjacent groups of arms is opposite, that is, $i_{b2} > 0$ and $i_{c1} < 0$, the two output voltages are just connected in the dead band, and there is no overlap, that is, no narrow pulse CMV will be formed.

Fig. 5(c) shows a dead-time compensation strategy achieving the elimination method of narrow pulse CMV caused by dead-time for NTM. Taking the arms group [a1, b2] and the currents polarity [$i_{a1} > 0$, $i_{b2} > 0$] as an example, set additional falling edge delay of gate signal S_{a1p} and rising edge delay of S_{a1d}, and the delay time is equal to dead time to realize the falling edge delay of output voltage u_{a1}. As a result, u_{a1} and u_{b2} no longer overlap, and the narrow pulse CMV can be eliminated. Similar to the implementation of eliminating the effect of dead time in [a1, b2], the elimination method of narrow pulse CMV generated by the dead time of the nose-to-tail gate signal in [a1, b2, c1, a2, b1, c2] is summarized in Table I. While the narrow pulse CMV caused by the dead time is removed, zero CMV can be fully implemented.

TABLE I
ELIMINATION METHOD OF NARROW PULSE CMV CAUSED BY DEAD TIME

Current polarity			Edge delay		
i_a	i_b	i_c	band	rising edge	falling delay
>0	**>0**	<0	[*a1*,*b2*], [*a2*,*b1*]	S_{a1d}, S_{a2d}	S_{a1p}, S_{a2p}
>0	**<0**	**<0**	[*b2*,*c1*], [*b1*,*c2*]	S_{c1d}, S_{c2d}	S_{c1p}, S_{c2p}
>0	<0	**>0**	[*c1*,*a2*], [*c2*,*a1*]	S_{c1p}, S_{c2p}	S_{c1d}, S_{c2d}
<0	**<0**	>0	[*a1*,*b2*], [*a2*,*b1*]	S_{b1p}, S_{b2p}	S_{b1d}, S_{b2d}
<0	**>0**	**>0**	[*b2*,*c1*], [*b1*,*c2*]	S_{b1d}, S_{b2d}	S_{b1p}, S_{b2p}
<0	>0	**<0**	[*c1*,*a2*], [*c2*,*a1*]	S_{a1p}, S_{a2p}	S_{a1d}, S_{a2d}

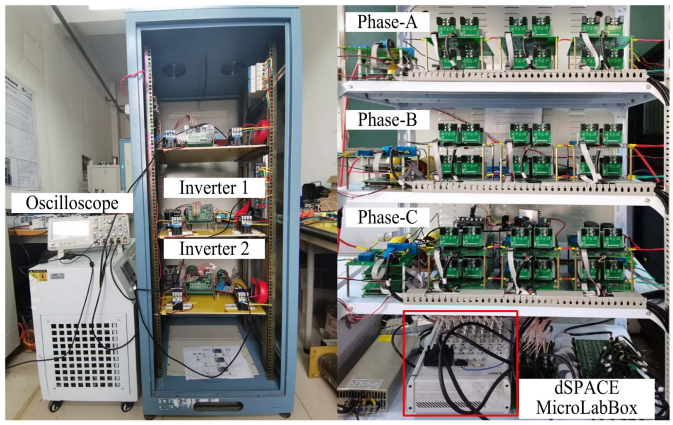

Fig. 6. Experimental prototype of (a) TPI and (b) MMC.

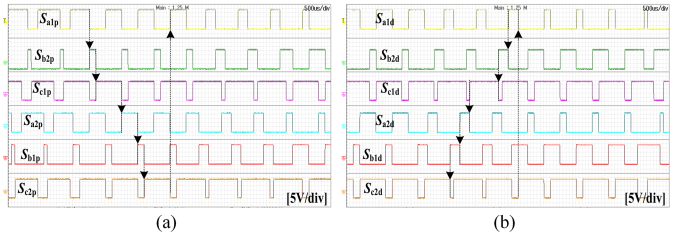

Fig. 7. Gate signal of NTM. (a) Upper arms group. (b) Lower arms group.

III. EXPERIMENTAL VERIFICATION

In order to further verify the effectiveness of the theoretical analysis of the proposed NTM method, both TPI and MMC experimental platforms are established in this letter, as shown in Fig. 6. The TPI platform shown in Fig. 6(a) consists of two inverters in parallel, and each arm in the MMC shown in Fig. 6(b) consists of two and four SMs, that is, both include 12*N* switching cells. The gate signal of upper and lower arms groups in TPI and MMC are shown in Fig. 7, the principle of which is the same as the diagram in Fig. 2.

A. TPI Verification

Fig. 8 shows the experimental results of TPI system with the modulation of SPWM and NTM. Fig. 8(a) and (b) shows the waveforms of phase-a1 pole voltage, inductor voltage, output phase-a voltage, and CMV with SPWM and NTM. Fig. 8(c)

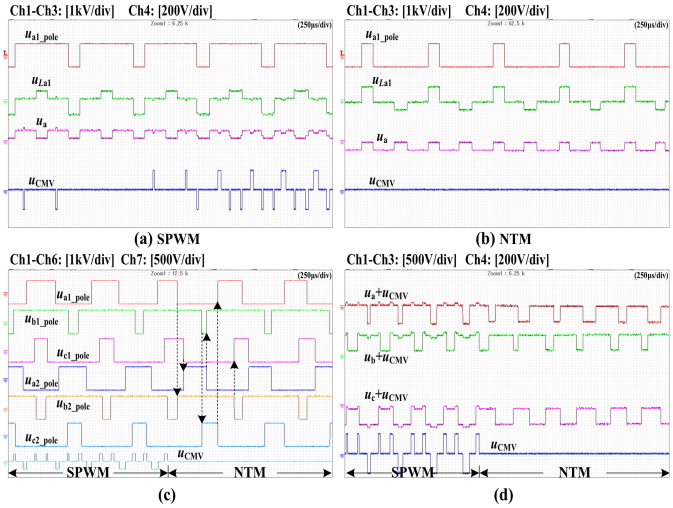

Fig. 8. Experimental results of phase-*a1* pole voltage, inductor voltage, output phase-*a* voltage, and CMV with (a) SPWM and (b) NTM. (c) Pole voltages of three legs and CMV. (d) Three-phase output voltages and CMV.

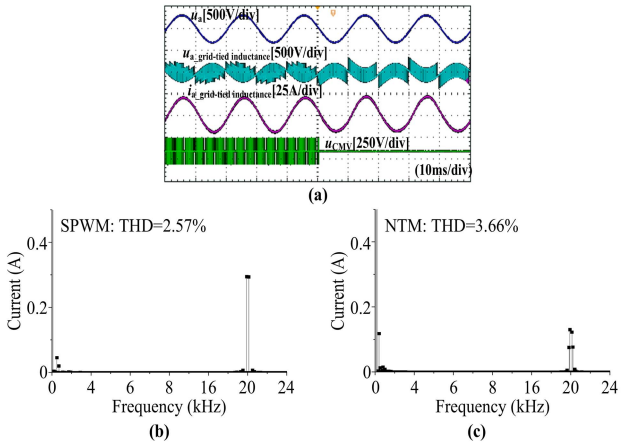

Fig. 9. Experimental results of the compromise between the CMV and THD with SPWM and NTM. (a) Grid voltage, grid-tied inductor current, grid-tied current, and CMV. Fast Fourier transform analysis of (b) SPWM and (c) proposed NTM.

shows the waveforms of pole voltages of three legs and CMV, and Fig. 8(d) presents the three-phase output voltages and CMV with SPWM and NTM. It can be seen from Fig. 8 that in SPWM, the peak-to-peak value of the CMV of TPI is 283 V. When the modulation method is switched to NTM, the CMV is only 3.7 V, basically realizing zero CMV completely. Fig. 9 shows the experimental results of the compromise between the CMV and total harmonic distortion (THD) with SPWM and NTM. While realizing zero CMV of TPI system, the proposed NTM method will increase harmonic voltage on grid-tied inductors to a certain extent, thus forming harmonic currents and resulting in the increase of THD. It can be seen from Fig. 9(b) and (c) that compared with SPWM, the THD of grid-tied current increased slightly from 2.57% to 3.66% in NTM.

Fig. 10 shows the experimental results of TPI operating in different conditions with NTM. No matter in the resistive operation of Figs. 8 and 9, or in the inductive operation shown

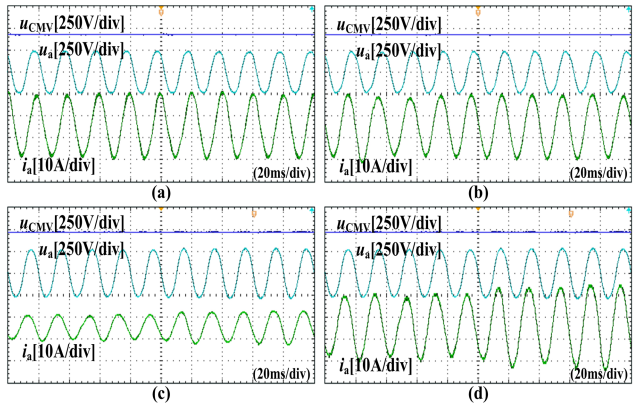

Fig. 10. Experimental results of TPI operating in different conditions with NTM. (a) Inductive operation. (b) Capacitive operation. Grid-tied active power (c) from 25% to 50% and (d) from 100% to 125% of capacitive operation.

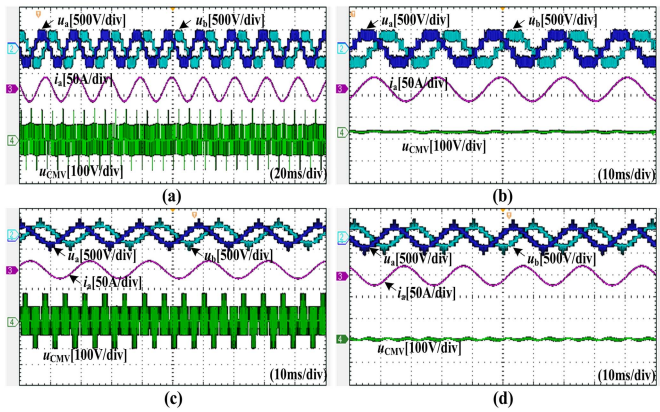

Fig. 11. Experimental results of MMC motor drive with (a) CPS-SPWM and (b) CPS-NTM of two SMs in one arm ($N = 1$), and (c) CPS-SPWM and (d) CPS-NTM of four SMs in one arm ($N = 2$). (a) CPS-SPWM, 5-level. (b) CPS-NTM, 5-level. (c) CPS-SPWM, 9-level. (d) CPS-NTM, 9-level.

in Fig. 10(a) and capacitive operation shown in Fig. 10(b), the proposed NTM can achieve zero CMV. Since it only changes the phase relationship between current and voltage when running in different quadrants, it does not affect the sequence relationship of the proposed voltage modulation, so it will not affect the elimination of CMV. Fig. 10(c) and (d) shows that under capacitive operation, when the grid-tied active power ranges from 25% to 50% and from 100% to 125%, the proposed NTM can realize zero CMV under continuous current mode.

B. MMC Verification

Fig. 11 shows the experimental results of MMC motor drive system with the modulation of CPS-SPWM and CPS-NTM. It can be seen that in SPWM shown in Fig. 11(a), the peak-to-peak value of the CMV of TPI is 282 V. When the modulation method adopts NTM shown in Fig. 11(b), the CMV is only 18.9 V, which is the third-order frequency CMV formed by the voltage fluctuations of the MMC SMs, and the high-frequency CMV formed by modulation has been almost completely eliminated. As shown in Fig. 11(c) and (d), in MMC of arm containing four SMs ($N = 2$), the proposed NTM can still achieve the zero CMV.

IV. Conclusion

The general condition of achieving zero CMV for three-phase dc/ac inverters with 12*N* switching cells at the modulation level is derived in this letter, based on which a novel NTM method is proposed. NTM recombines and resorts the 12*N* units, and places the gate signal nose-to-tail of the six switching cells in the upper/lower arm. Finally, the numbers of switch-ON/OFF cells of the upper and lower arms are exactly the same at any time, thus realizing zero CMV. In addition, an elimination method of narrow pulse CMV caused by dead time is also designed for NTM.

References

[1] S. Jain, A. K. Thopukara, R. Karampuri, and V. T. Somasekhar, "A single-stage photovoltaic system for a dual-inverter-fed open-end winding induction motor drive for pumping applications," *IEEE Trans. Power Electron.*, vol. 30, no. 9, pp. 4809–4818, Sep. 2015.

[2] M. Wu and R. Zhao, "Method analysis and comparison of SVPWM and SPWM," in *Proc. IEEE 29th Chin. Control Conf.*, 2010, pp. 3184–3187.

[3] Z. Ke et al., "Capacitor voltage ripple estimation and optimal sizing of modular multi-level converters for variable-speed drives," *IEEE Trans. Power Electron.*, vol. 35, no. 11, pp. 12544–12554, Nov. 2020.

[4] J. Teng et al., "Two types of common-mode voltage suppression in medium voltage motor speed regulation system based on solid state transformer with dual DC bus," *IEEE Trans. Power Electron.*, vol. 37, no. 6, pp. 7082–7099, Jun. 2022.

[5] M. Wu, C. Xue, Y. W. Li, and K. Yang, "A generalized selective harmonic elimination PWM formulation with common-mode voltage reduction ability for multilevel converters," *IEEE Trans. Power Electron.*, vol. 36, no. 9, pp. 10753–10765, Sep. 2021.

[6] L. Weiwei et al., "Integrated modulation of dual-parallel three-level inverters with reduced common mode voltage and circulating current," *IEEE Trans. Power Electron.*, vol. 36, no. 11, pp. 13332–13344, Nov. 2021.

[7] Z. Shen, D. Jiang, T. Zou, and R. Qu, "Dual-segment three-phase PMSM with dual inverters for leakage current and common-mode EMI reduction," *IEEE Trans. Power Electron.*, vol. 34, no. 6, pp. 5606–5619, Jun. 2019.

[8] S. Du, B. Wu, and N. Zargari, "Common-mode voltage minimization for grid-tied modular multilevel converter," *IEEE Trans. Ind. Electron.*, vol. 66, no. 10, pp. 7480–7487, Oct. 2019.

[9] A. Edpuganti and A. K. Rathore, "Optimal pulsewidth modulation for common-mode voltage elimination scheme of medium-voltage modular multilevel converter-fed open-end stator winding induction motor drives," *IEEE Trans. Ind. Electron.*, vol. 64, no. 1, pp. 848–856, Jan. 2017.

[10] G. D. Holmes, T. A. Lipo, and T. A. Lipo, *Pulse Width Modulation For Power Converters: Principles and Practice*. Hoboken, NJ, USA: Wiley-IEEE Press, 2003.